Molecular dynamics and free energy perturbation studies of Ca²⁺/Sr²⁺ complexation selectivities of the macrocyclic ionophores DOTA and TETA in water

Alexandre Varnek,[a] Georges Wipff,*[a] Alex Bilyk[b] and Jack M. Harrowfield[b]

[a] *Laboratoire MSM, UMR 7551 CNRS, Institut de Chimie, 4, rue B. Pascal, 67 000 Strasbourg, France*
[b] *Department of Chemistry, University of Western Australia, Nedlands, 6907, Western Australia*

Molecular dynamics simulations have been performed on the uncomplexed tetraanionic macrocyclic ionophores DOTA **I** and TETA **II** and on their complexes with Ca²⁺ and Sr²⁺ cations in the gas phase and in water. We have found that for both ligands, the most stable complex is the one where the cation is completely encapsulated in a pseudocavity formed by four nitrogens and four oxygens (one per carboxylate group). All stereoisomers for this type of complex have similar coordination and hydration patterns. Water molecules do not coordinate to the cation when it is encapsulated by the ligand but form hydrogen bonds with non-coordinating carboxylic oxygens, leading to repulsive interactions with the cation. The higher binding affinity of **I** compared to **II** for Ca²⁺ is explained by better preorganization of **I** for complexation. Free energy perturbation simulations performed on **I**·M²⁺ and **II**·M²⁺ complexes show that the preference of both ligands for Ca²⁺ over Sr²⁺ in water results from their higher intrinsic binding affinities for Ca²⁺ rather than the difference between hydration energies of the uncomplexed cations.

Introduction

Since the early demonstration by Desreux *et al.*[1–3] of the remarkable characteristics of the rare earth metal ion complexes of the functionalized macrocycle, 1,4,7,10-tetracarboxymethyl-1,4,7,10-tetraazacyclododecane, "DOTA-H₄", intense interest has developed in the coordination chemistry of this ligand, its homologs and their various derivatives.[4] Much of this has centered on potential applications of the gadolinium(III) complexes, in particular, as relaxivity enhancement agents for magnetic resonance imaging.[5–8] Spectroscopic studies performed on the complexes of DOTA tetraanion (**I**, Chart 1)
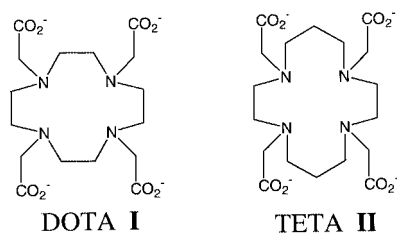
Chart 1

with lanthanides (Ln³⁺) in water[9–11] show that the metal cation coordinates to four oxygens and to four nitrogens of the ligand, whereas a ninth coordination place is occupied by one water molecule which is rapidly exchanging with the bulk solvent. It has been also shown that an equilibrium of four stereoisomers M_1, M_2, m_1 and m_2 of the **I**·Ln³⁺ complexes takes place (Fig. 1). These forms differ by the helicity of the macrocyclic ring and/or of the acetate arms; M_1 and M_2 are enantiomers as are m_1 and m_2.

It is well known that there are many close parallels in the coordination chemistry of the tripositive rare earths and calcium(II),[12–14] and the DOTA tetraanion is in fact generally considered the most effective calcium ion complexant yet known.[3,15–17] In the context of searching for selective extraction agents for the alkaline earth metal ions, we were concerned to
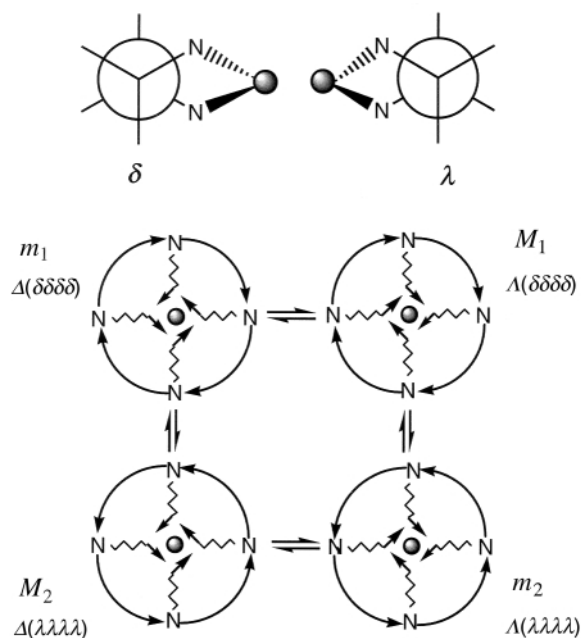
Fig. 1 *Top*: enantiomers δ and λ of the ethylene diamine fragments complexed with a metal cation. *Bottom*: schematic representation of the M_1, M_2, m_1 and m_2 stereoisomers of the **I**·Ca²⁺ complex. Additionally, for each stereoisomer a denomination according to IUPAC rules[48,49] is given. The symbols Λ and Δ correspond, respectively, to the clockwise and counter-clockwise helicity of acetate arms, whereas $\delta\delta\delta\delta$ and $\lambda\lambda\lambda\lambda$ account for the helicity of the macrocyclic backbone. Orientations of the C=O groups tangential to the cation and relative helicity of the macrocyclic ring are shown by arrows.

find explanations for both the selectivity of calcium binding to **I** over the homolog TETA, the tetraanion of 1,4,7,10-tetracarboxymethyl-1,4,7,10-tetraazacyclotetradecane (**II**, Chart 1)[1–3] and the selectivity of **I** and **II** for Ca²⁺ over Sr²⁺.[17] Therefore we conducted molecular modeling studies on these ligands and

their complexes with Ca^{2+} and Sr^{2+} to gain some insights of the factors which may be most important in determining complexation selectivities and to provide a basis for developing a better understanding of systems involving alkaline earth cations.

Analysis of available solid state structural data for complexes of $\mathbf{I}$ [18] shows that coordination patterns of Ca^{2+} (eight coordinated) differ from those found for tripositive rare earth cations (nine coordinated). A problem associated with the use of such data as an initial reference point for our modeling studies is that the cation encapsulated by $\mathbf{I}$ is in all cases accompanied by a second cation interacting to some extent with the $\mathbf{I}$ carboxylate groups and therefore presumably having some influence upon the observed structure. Nonetheless, studies [1] of $[Eu \cdot \mathbf{I} \cdot H_2O]^-$ in aqueous solution (where presumably any association with its sodium counterion is negligible) by ^1H nuclear magnetic resonance spectroscopy have shown exceptionally good agreement between the solid state and solution structures.

Earlier, quantum mechanics [19] and force field [20–25] simulations of rare earth metal complexes of $\mathbf{I}$ and related ligands have been performed, but no theoretical results on complexes with alkaline-earth cations in solution are yet available. In this paper we report molecular dynamics (MD) and free energy simulations in the gas phase and in water of the complexes of $\mathbf{I}$ and $\mathbf{II}$ with Ca^{2+} and Sr^{2+}, trying to gain microscopic insights into the structure of complexes and observed complexation selectivity of studied macrocyclic ligands. More specifically, we focused on the following questions: (*i*) are the structures of complexes simulated in the gas phase and in water similar to those found experimentally in the solid sate, (*ii*) are there any differences between coordination and hydration patterns of the complexes with lanthanides and with alkaline-earth cations? (*iii*) why do $\mathbf{I}$ and $\mathbf{II}$ ligands complex Ca^{2+} better than Sr^{2+} in water, and, (*iv*) why is $\mathbf{I}$ a better Ca^{2+} binder than $\mathbf{II}$?

2 Method

The AMBER 4.1 program [26] was used for molecular mechanics, molecular dynamics and free energy simulations, with the following representation of the potential energy:

$$E_T = \Sigma_{bonds} K_r (r - r_{eq})^2 + \Sigma_{angles} K_\theta (\theta - \theta_{eq})^2 +$$
$$\Sigma_{dihedrals} V_n/2(1 + \cos n\varphi) +$$
$$\Sigma_{i<j}(q_i q_j/R_{ij} + \varepsilon_{ij}(R_{ij}^*/R_{ij})^{12} - 2\varepsilon_{ij}(R_{ij}^*/R_{ij})^6)$$

The bonds and bond angles are treated as harmonic springs with force constants K_r and K_θ, respectively, and a torsional term is associated with dihedral angles and a barrier to rotation V_n. The interactions between atoms separated by at least three bonds are described with a pairwise additive 12-6 potential defined by the parameters ε and R^*, and a coulombic term is calculated using atomic charges q_i.

Fitting of parameters

The van der Waals parameters for atoms of $\mathbf{I}$ and $\mathbf{II}$ were taken from the AMBER force field [27] using the atom types given in Fig. 2. For Ca^{2+} initially we took the same AMBER parameters as for the Na^+ cation, then other sets of parameters were systematically tested. Electrostatic potential charges were initially calculated for the $Me_2N-CH_2-COO^-$ fragment with the Spartan 4.1 program [28] using the 6-31G* basis set. When this initial set of parameters for non-bonded interactions was used in the gas phase minimizations of $\mathbf{I} \cdot Ca^{2+}$, the $Ca^{2+}-O$ distances were found to be too small (2.07–2.33 Å) whilst the $Ca^{2+}-N$ distances (2.90–3.06 Å) were too large compared to the reported crystal structure ($Ca^{2+}-O = 2.40$ Å, $Ca^{2+}-N = 2.58$ Å). To reproduce cation–ligand coordination bond distances obtained from experimental results, different sets of charges and van der Waals parameters were tested. The original charges for the O (-0.87) and N (-0.47) obtained from *ab initio* calculations were systematically modified by increasing the charges
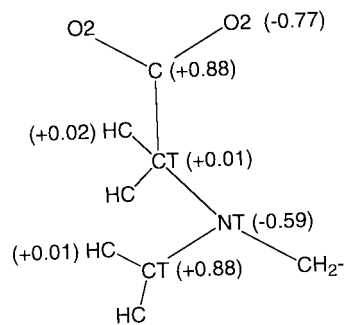

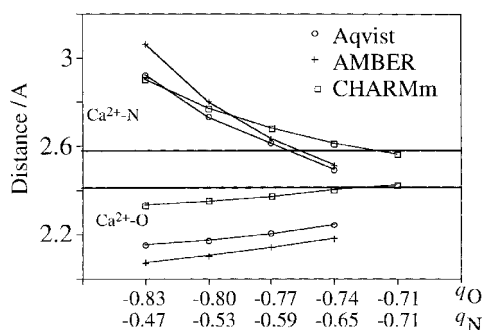**Fig. 2** Atomic charges and AMBER atomic types used in molecular dynamics simulations.

Fig. 3 $Ca^{2+}-N$ and $Ca^{2+}-O$ distances for $\mathbf{I} \cdot Ca^{2+}$ as a function of N and O charge. The van der Waals parameters Ca^{2+} investigated were obtained from Åqvist ($R^* = 1.3261$, $\varepsilon = 0.44957$),[32] CHARMm ($R^* = 1.71$, $\varepsilon = 0.12$)[33] and AMBER force fields ($R^* = 1.87$, $\varepsilon = 0.0028$).[26] The lower horizontal line indicates the $Ca^{2+}-O$ distance observed in the solid state and the upper one represents the $Ca^{2+}-N$ distance.

on N and decreasing the charge on O whilst the charges on C and H remained the same (Fig. 3). As shown qualitatively in the QM/MM calculations [29] such modifications of the charges mimic polarization effects.[30] The charge polarization in the model EDTA ligand, also containing the $N-CH_2-COO^-$ fragment, has recently been assessed by quantum mechanical calculations, in which a point charge of $+1$, $+2$ and $+3$ was placed at the cation position of the $EDTA \cdot Eu^{3+}$ complex. The corresponding Mulliken charges obtained with a 6-31 G* basis set were ($q_N = -0.56$, $q_O = -0.79$), ($q_N = -0.70$, $q_O = -0.82$) and ($q_N = -0.84$, $q_O = -0.85$), respectively.[31] Four sets of atomic charges of $\mathbf{I}$ were combined with three sets of van der Waals parameters for Ca^{2+}: (*i*) Na^+-like potentials from Åqvist ($R^* = 1.87$ Å, $\varepsilon = 0.0028$ kcal mol^{-1}),[32] (*ii*) Åqvist parameters ($R^* = 1.3261$ Å, $\varepsilon = 0.44957$ kcal mol^{-1})[32] and CHARMm parameters ($R^* = 1.71$ Å, $\varepsilon = 0.12$ kcal mol^{-1}).[33] A series of gas phase minimizations, starting from the solid state structure of $\mathbf{I} \cdot Ca^{2+}$ determined that charges of -0.77 for O and -0.59 for N and the CHARMm parameters [33] for Ca^{2+} provided the best agreement with the solid state distances (Fig. 3). Åqvist [32] "sodium" and "calcium" parameters for Ca^{2+} were also investigated but proved to be unsatisfactory as the Ca–O bond distances were always too short. Finally selected charges for the simulations in this work are given in Fig. 2. The C and H atoms of the two extra methylene groups in $\mathbf{II}$ were given the charges of -0.04 and $+0.02$ respectively. In the MD simulations of the $\mathbf{L} \cdot Sr^{2+}$ complexes, we used the CHARMm van der Waals parameters for Sr^{2+} ($R^* = 1.977$, $\varepsilon = 0.1717$ kcal mol^{-1})[33] in order to be consistent with the representation of the $\mathbf{L} \cdot Ca^{2+}$ complexes.

Using the free energy perturbation technique and CHARMm van der Waals parameters for M^{2+}, we calculated the difference between free energies of hydration of Ca^{2+} and Sr^{2+}. The calculated value of ΔG_3 (37.3 kcal mol^{-1}) obtained for the system including a cation and 714 water molecules,

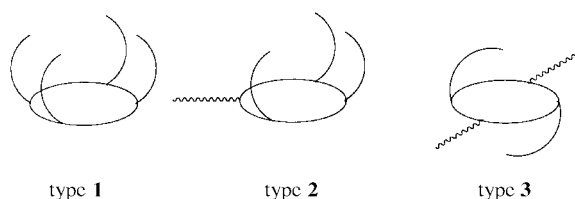<center>type **1**   type **2**   type **3**</center>

Fig. 4 Representation of three possible ligand binding modes for complexation with M^{2+}.

agrees reasonably well with the experimental one (34.9 kcal mol^{-1}).[32] Thus, a choice of the CHARMm parameters for Ca^{2+} and Sr^{2+} looks quite reasonable both from the structural and the energetic point of view.

Preparation of starting structures

Simulations were performed on two groups of conformers of **I** and **II** differing either by the number of coordinating carboxylate groups, or by the helicity of the macrocyclic backbone and/or of the acetate arms. In the available solid state structure of **I**·$2Ca^{2+}$,[34] the encapsulated cation is situated inside the pseudo-cavity formed by four nitrogens of the macrocyclic backbone and four oxygens of the lateral carboxylate groups. One can assume that in aqueous solution some of the oxygens of carboxylate groups can be replaced by solvent molecules. In fact, conformational sampling of the complexes of tetraanions **I** and **II** with M^{2+} in water is a difficult task because of strong cation–ligand electrostatic interactions and, hence, high kinetic barriers separating different conformers. Therefore, we have prepared three typical starting structures, **1**, **2** and **3** which correspond to four, three or two carboxylates bound to the cation, respectively (Fig. 4).

For the two starting structures **1** and **2** of the **I**·M^{2+} complex, we used, respectively, the available solid state structure[34] and one built with the MacroModel program.[35] For the **II**·M^{2+} complexes three conformational types **1**–**3** were studied. The starting structures of type **1** were obtained from the solid state structure of the **II**·Tb^{3+} complex[36] by replacing the Tb^{3+} with Ca^{2+} or Sr^{2+}. The **II**·Ca^{2+} (type **2**) starting structure was built using MacroModel.[35] A structure of the type **3** for **II**·Ca^{2+} was prepared using solid state X-ray data for the **II**·Zn^{2+} complex.[37] The starting structures for the free ligands were obtained either by removing the metal ion from the complexes or from conformational searching in the gas phase by the Monte Carlo procedure[38] performed with the MacroModel program.[35] For the type **3** complexes, only **II**·M^{2+} were simulated because the macrocyclic cavity of **I** is too small for the incorporation of M^{2+} within the plane of its nitrogens.

According to notation given in reference 10, the **I**·Ca^{2+} (type **1**) complex found in the solid state structure[34] is of M_I type. Stereoisomer m_2 of this complex was prepared with the MacroModel program, using solid state data for the complex La(DOTAM)   (DOTAM = 1,4,7-tetrakis(2-carbamoylethyl)-1,4,7,10-tetraazacyclododecane)[39] which has a tetraazacyclododecane backbone, as in the molecule **I**, but with different helicity (Fig. 1). For the type **1** complexes of **II**, only the M_I form has been studied.

Simulations protocol

The scaling factor 1/2 was used to reduce $1 \cdots 4$ non-bonded interactions. For the solvent, TIP3P model for water was used.[40] All complexes were first energy minimized *in vacuo* before being immersed in solution. The solvent boxes were of 34 Å to 39 Å length and contained from 1355 to 1542 water molecules, simulated with periodic boundary conditions imposed. The solute was placed at the center of the box and all solvent molecules within 2 Å of the solute were deleted. In solution, the C–H bonds were constrained to constant values with SHAKE, in conjunction with a time step of 2 fs.

After 1000 steps of conjugate gradient energy minimization, the MD simulations were run for 300–500 ps unless stated otherwise in the text, at 300 K in a (N, P, T) ensemble using the Verlet algorithm, starting with random velocities. A residue based twin cut-off of 11/14 Å was used for non-bonded interactions. The temperature was controlled by velocity scaling in the gas phase, and by coupling to a thermal bath in solution with a relaxation time of 0.1 ps.

The "FEP" (free energy perturbation) calculations were performed with the windowing technique, changing the ε, R^* parameters of M^{2+} linearly with λ, as suggested:[41] $\varepsilon_\lambda = \lambda \cdot \varepsilon_{Ca}^{2+} + (1 - \lambda) \cdot \varepsilon_{Sr}^{2+}$; $R^*_\lambda = \lambda \cdot R^*_{Ca}^{2+} + (1 - \lambda) \cdot R^*_{Sr}^{2+}$. The mutation $Ca^{2+} \rightarrow Sr^{2+}$ was achieved in 21 windows. At each window, 1 ps of equilibration was followed by 4 ps of data collection, and the change of free energy ΔG was averaged from the forward and backward cumulated values. The change in ΔG from Ca^{2+} to Sr^{2+} was obtained from the cumulated free energies involved in the intermediate states.

Analysis of results

The interaction energies, cation–ligand ($E_{M \cdots L}$), cation–solvent ($E_{M \cdots w}$), ligand–solvent ($E_{L \cdots w}$), solvent–solvent ($E_{w \cdots w}$), and intrinsic energies of the ligand (E_L) were recalculated from the MD trajectories using the MD_DRAW program.[42] The energy fluctuations are typically 3–10 for $E_{M \cdots L}$, $E_{M \cdots w}$ and E_L, 25–30 for $E_{L \cdots w}$ and 40–55 kcal mol^{-1} for $E_{w \cdots w}$ and for the total energy of the system. The radial distribution functions (RDF) of the carboxylate oxygen atoms, nitrogens and Ca^{2+} were calculated in water. The number of solvent molecules coordinated to these atoms was obtained by integration of the first peak of the RDF.

3 Results and discussion

3.1 Free ligands in the gas phase and in water

In the gas phase, structures of uncomplexed **I** and **II** ligands found in the Monte-Carlo conformational search (**MC**) with the MacroModel program[35] are more stable than those simulated starting from the "organized" type **1** and **2** forms. All conformers are "flattened" because of electrostatic repulsion of the carboxylatomethyl arms, but the geometry of the macrocyclic backbone also differs. The **MC** conformers display an alternative "up"–"down" orientation of the nitrogen lone pairs, whereas in type **1** all of them are "up", and in type **2** three lone pairs are oriented "up", and one is "down".

In water, the type **1** and **2** conformers of the **I** and **II** ionophores relax to much less flattened forms than in the gas phase. As a result, their conformational energies E^0_L (Table 1) are 20–40 kcal mol^{-1} higher than for the **MC** gas phase structures (404 and 395 kcal mol^{-1} for **I** and **II**, respectively). This extra strain is compensated by favourable solute–solvent interactions (Table 1).

The relative stability of different conformers of uncomplexed **L** depends on differences in their total energies, E_{tot}, which include conformational energy E^0_L, hydration energy $E^0_{L \cdots w}$ and water–water interaction energy $E_{w \cdots w}$ contributions.

$$E_{tot} = E^0_L + E^0_{L \cdots w} + E_{w \cdots w} \qquad (1)$$

Direct calculations of ΔE_{tot} are not reasonable because of large fluctuations in the computed water–water interaction energies and the different number of solvent molecules in the simulation box (Table 1). However, due to small variations in water–water interaction energy per H_2O molecule E^1_{wat} in simulated systems (Table 1), we assume that the $E_{w \cdots w}$ term is similar for different forms of **I** or **II**. In this case, the sum of the first two terms in eqn. (1) can be used as a criterion of relative stability of different conformers.

Table 1 Average energy components (kcal mol⁻¹) of the macrocyclic ligands **I** and **II** in water[a]

Ligand	Type of conformation[b]	E^0_L	$E^0_{L\cdots W}$	E^0_{LW}	$E_{W\cdots W}$	N	E^1_{wat}[c]
I	**1**	446(6)	−963(28)	−517	−12704(47)	1360	9.34
	2	447(7)	−973(29)	−526	−12658(61)	1355	9.34
	MC	429(6)	−932(27)	−503	−12964(45)	1385	9.36
II	**1**	453(10)	−974(29)	−521	−12932(50)	1384	9.34
	2	428(9)	−926(29)	−498	−14496(54)	1542	9.40
	MC	422(8)	−909(27)	−487	−14102(50)	1501	9.40

[a] Conformational energies (E^0_L, kcal mol⁻¹), solute–solvent interaction energies ($E^0_{L\cdots W}$), "total" energies of solute ($E^0_{LW} = E^0_{L\cdots W} + E^0_L$), and water–water interaction energies (kcal mol⁻¹) of uncomplexed **I** and **II** in water. Statistical fluctuations are given in parentheses. [b] The starting structures correspond to the conformation **1** and **2** of **I** and **II** in their complexes with Ca²⁺, or to the lowest energy conformers obtained from Monte Carlo search (**MC**) in the gas phase. [c] Average water–water interaction energy per one H₂O molecule, $E^1_{wat} = E_{W\cdots W}/N$, where N is the number of water molecules.

$$E^0_{LW} = E^0_L + E^0_{L\cdots W} \qquad (2)$$

Comparing the E^0_{LW} energies, one may conclude that the conformers of the free ligands derived from the **L·M²⁺** complexes (type **2** for **I** and type **1** for **II**) are more stable in water than those obtained from the "best" gas phase structures. Thus, water plays an important organizing role "preparing" **L** for complexation. Integration of the RDF O···H_W and N···H_W for studied forms of the free ligands show that each carboxylate oxygen is hydrogen bonded on average to three water molecules whilst each nitrogen coordinates to one water molecule only.

3.2 I·Ca²⁺ and II·Ca²⁺ complexes in the gas phase and in water

Type 1 complexes. Most of the calculations have been performed on the stereoisomer M_1 (Fig. 1) of the **I·Ca²⁺** complex. In the gas phase, as in water, **I·Ca²⁺** (M_1) represents a distorted square antiprism (Fig. 5). The plane defined by the coordinated oxygens is almost parallel to the plane of the nitrogens, the angle between them being 9°. In the gas phase, the Ca²⁺ is much closer to the plane of the coordinated oxygens (0.9 Å) than to the plane of the nitrogens (1.7 Å).

The coordination patterns in the **II·Ca²⁺** (M_1) complex are similar to **I·Ca²⁺**. The Ca²⁺–N distances are slightly longer (by 0.15 Å) than those in **I·Ca²⁺** whereas the Ca²⁺–O distances are almost identical (Table 2). Unlike the **I·Ca²⁺** complex, the nitrogens of **II·Ca²⁺** (type **1**) do not lie exactly in the same plane: two opposite nitrogens lie 0.2 Å above, and the other two lie below the average plane of all N atoms. Analogously, a shift from coplanarity is observed for the coordinated oxygens, similarly to the solid state **II·Tb(III)** structure.[36]

In water, simulated M_1 stereoisomers of **I·Ca²⁺** and **II·Ca²⁺** are similar to the gas phase structures (Fig. 5 and Table 2). Ca²⁺–O distances are slightly larger (by 0.03 Å) whilst Ca²⁺–N distances are shorter (by 0.16 Å) and the Ca²⁺ moves slightly deeper into the pseudocavity of the ligand, a trend observed during most of the simulations in water except that of **II·Ca²⁺** (type **3**). The shape of the complexes and cation–donor atoms distances (Table 2) are similar for **I·Ca²⁺** and **II·Ca²⁺**, explaining why cation–ligand interaction energies in both complexes are similar (Table 3). No conformational transformations have been observed for 300 ps of simulations.

The m_2 stereoisomer of **I·Ca²⁺** was modeled in the gas phase and in water. The Ca²⁺–N and Ca²⁺–O distances are almost identical to those found for the M_1 form. In the gas phase, no conformational exchange has been observed during 500 ps of simulations. In water, the m_2 form passed into the M_2 form in 135 ps after the beginning of simulations, and remained unchanged until the end of 500 ps of MD. Simulations of the same duration on the M_2 stereoisomer did not lead to any conformational transformations.

MD simulations were also performed on the neutral **I·2Ca²⁺** complex starting from the solid state structure[34] with

Table 2 Complexes **L·M²⁺** (**L** = **I**, **II**; M²⁺ = Ca²⁺, Sr²⁺) in the gas phase and in water: average M²⁺–O and M²⁺–N distances (Å)[a]

Ligand	Type	In the gas phase		In water	
		M²⁺–N	M²⁺–O	M²⁺–N	M²⁺–O
Ca²⁺ complexes					
I	**1**[d]	2.72	2.39	2.58	2.42
	2	2.61	2.36	2.58, 2.72[c]	2.41
II	**1**	2.87	2.37	2.67	2.42
	2	2.62, 4.55[b]	2.37	2.58, 2.72[c]	2.39
	3	2.48	2.34	2.53	2.42
Sr²⁺ complexes					
I	**1**	2.62	2.89	2.67	2.82
II	**1**	2.60	2.95	2.66	2.89

[a] Within each complex all cation–donor atom distances are similar within statistical fluctuations (±0.02 Å) except [b] for **II** (type **2**) in the gas phase, where two N atoms are strongly bound and the other two weakly bound to Ca²⁺, and, [c] for **I** (type **2**) and (**II** type) **2** in water, where the Ca²⁺–N distance for the N atom directly connected to the non-coordinating carboxylate arm is longer. [d] For all stereoisomers of **I·Ca²⁺** (type **1**) related distances are similar within statistical fluctuations.

one cation coordinated in *exo* fashion and another one in *endo* fashion. In the course of simulations, this complex rapidly dissociated into **I·Ca²⁺** and Ca²⁺ species.

Type 2 complexes. In the gas phase, the cation in **I·Ca²⁺** coordinates four nitrogens and three oxygens. The nitrogen connected to the uncoordinated carboxylatomethyl arm is slightly further away from the metal. In the **II·Ca²⁺** complex, the coordination sphere of Ca²⁺ includes six O and two N atoms. Two of the coordinating carboxylates are bound to calcium by only one of their oxygens, as in **I·Ca²⁺**, whilst the other binding carboxylate is bound to the metal by both its oxygens.

In water, the structure of the **I·Ca²⁺** complex is similar to that in the gas phase (Fig. 5, Table 2). The coordination number of Ca²⁺ has changed from seven in the gas phase, to eight in water since one solvent molecule binds to the cation. The **II·Ca²⁺** complex significantly changes during the MD simulation in water (Fig. 5). Only unidentate coordination from all three binding carboxylates is observed, Ca²⁺–N distances in **II·Ca²⁺** are similar to the corresponding distances found in **I·Ca²⁺** and all four nitrogens are bound to Ca²⁺. Unlike **I·Ca²⁺** (type **2**), no solvent molecule coordinates to the cation in **II·Ca²⁺** (type **2**).

Type 3 complexes. In the **II·Ca²⁺** complex, the cation has an octahedral environment (Fig. 5). In the gas phase simulations Ca²⁺ lies in the plane of the nitrogens forming Ca²⁺–N coordination bonds (2.34 Å) shorter than in type **1** and **2** complexes (2.62–2.87 Å). The Ca²⁺–O distances are similar to those in the complexes of other types. In water, one water molecule
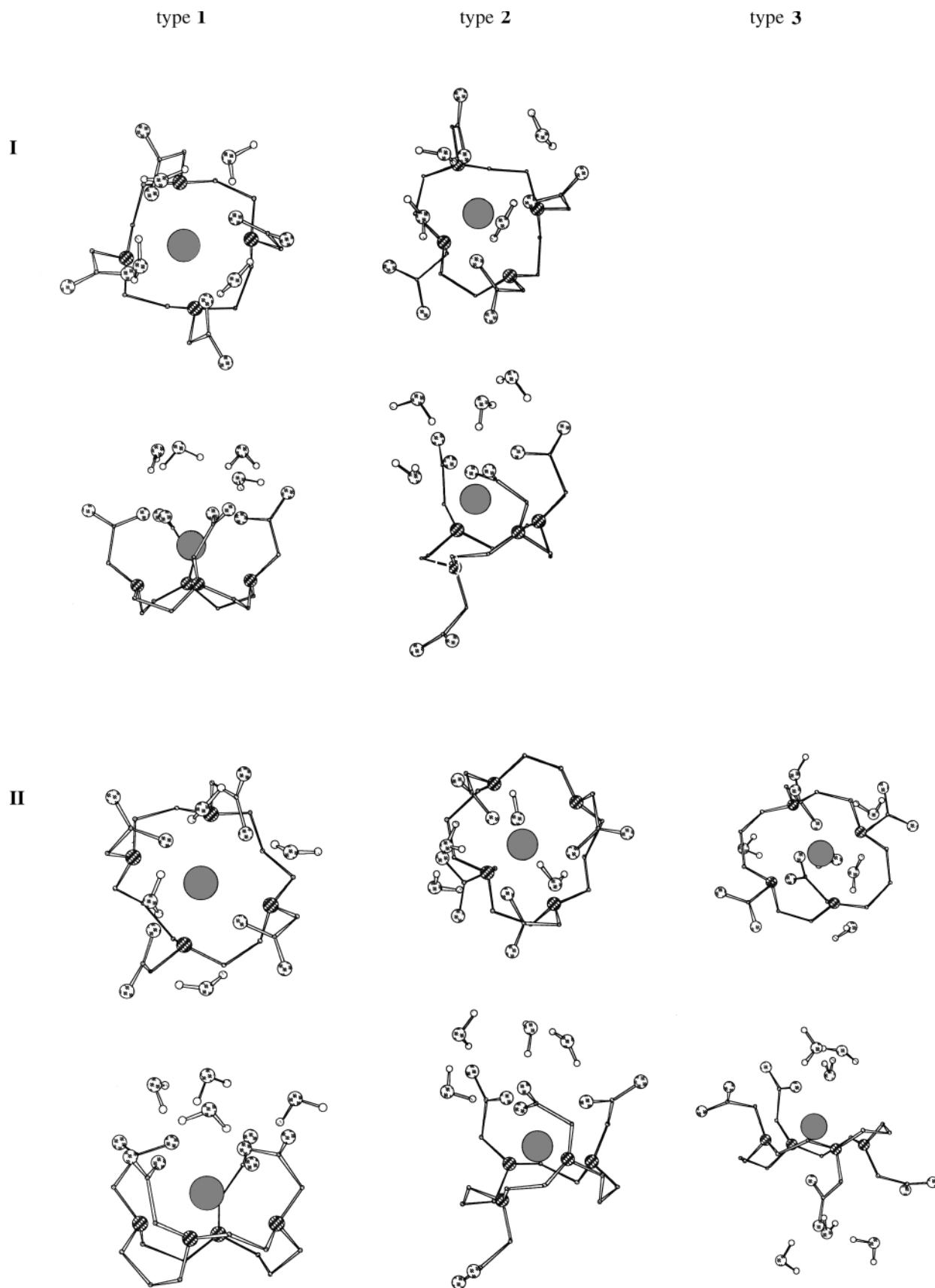
Fig. 5 Structure of **I**·Ca²⁺ and **II**·Ca²⁺ complexes with selected water molecules after 300 ps of molecular simulations. For each structure: top view (first line) and side view (second line).

coordinates to the cation in **II**·Ca²⁺ (type **3**), pulling Ca²⁺ by 0.6 Å from the plane of the nitrogens (Fig. 5).

Relative stability of different conformers of the complexes in water. Due to small variations in water–water interaction energy per one H_2O molecule in simulated systems (Table 3), as for the simulations on free ligands, we assume that the water–water interaction energies are similar for different forms of the **L**·Ca²⁺ complexes. In this case, the "total" energy of the complexes, E_{MLW}, which is a sum of the conformational energy

Table 3 Average energy components (kcal mol⁻¹) of the M²⁺·L (M²⁺ = Ca²⁺, Sr²⁺, L = I, II) complexes in water [a,e]

Ligand	Type of complex	E_L	$E_{M\cdots L}$	E_{ML}	$E_{L\cdots w}$	$E_{M\cdots w}$[b]	$E_{ML\cdots w}$[c]	E_{MLW}[d]	$E_{w\cdots w}$	N	$E^1_{w\cdots w}$
Ca²⁺ complexes											
I	**1** *M* form	610	−972	−362	−623	215	−408	−770	−13006	1361	−9.57
	1 *m* form	627	−979	−352	−627	218	−409	−761	13000	1358	−9.57
	2	547	−885	−338	−555	146	−409	−747	−13107	1370	−9.57
II	**1**	658	−973	−315	−656	216	−440	−755	−13228	1384	−9.56
	2	577	−890	−313	−519	181	−408	−721	−14328	1495	−9.56
	3	528	−816	−288	−533	101	−432	−720	−14775	1542	−9.58
Sr²⁺ complexes											
I	**1**	564	−880	−316	−573	179	−394	−710	13020	1361	−9.57
II	**1**	605	−880	−275	−630	206	−424	−699	13229	1384	−9.56

[a] See definitions in Tables 1 and 2. Statistical fluctuations are 7–8 for $E_{M\cdots L}$ and E_L, 15–20 for $E_{M\cdots w}$, 25–30 for $E_{L\cdots w}$ and 45–50 kcal mol⁻¹ for $E_{w\cdots w}$. [b] Cation–water ($E_{M\cdots w}$) and [c] complex–water ($E_{ML\cdots w}$) interaction energies. [d] $E_{MLW} = E_{ML} + E_{ML\cdots w}$. [e] If not specified, simulations are performed on the M_I forms of the type **1** complexes.
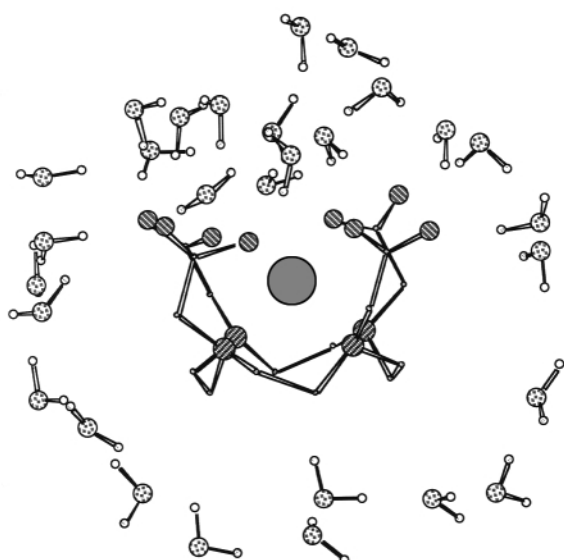

Fig. 6 Hydrophobic and hydrophilic regions for **I**·Ca²⁺ (type **1**) after 300 ps of simulation time. Selected water molecules within 6.9 Å of the center of mass of **I**·Ca²⁺ (type **1**) are shown (water molecules in front of or behind the solute have been removed for clarity).

of ligands E_L, cation–ligand interaction energy $E_{M\cdots L}$, and hydration energy of the complex $E_{ML\cdots w}$, can be used as a

$$E_{MLW} = E_L + E_{M\cdots L} + E_{ML\cdots w} \qquad (3)$$

criterion of relative stabilities of different conformers. The E_{MLW} values and their components given in Table 3 show that in water, type **1** is the most stable form of **L**·Ca²⁺. Thus, for the **I**·Ca²⁺ complex, conformer **1** is 23 kcal mol⁻¹ more stable than conformer **2** because of more favourable cation–ligand interactions. A similar trend is observed for **II**·Ca²⁺, where form **1** is 32 kcal mol⁻¹ more stable than **2** and 34 kcal mol⁻¹ more stable than **3**. Interestingly, the forms **1** and **2** of **I**·Ca²⁺ are similarly hydrated (Table 3). This results from a compensation of two opposite effects: in **1** cation–water interactions are more repulsive than in **2**, but the ligand itself is better hydrated. Repulsive Ca²⁺–water interactions result from orientation of the first shell water molecules which form strong hydrogen bonds with the oxygens of the carboxylate groups.

Energy components given in Table 3 show that stereoisomers *m* of the **I**·Ca²⁺ (type **1**) complex are intrinsically less stable than the *M* forms, because of larger ligand strain energy. Hydration energies of the two forms are similar.
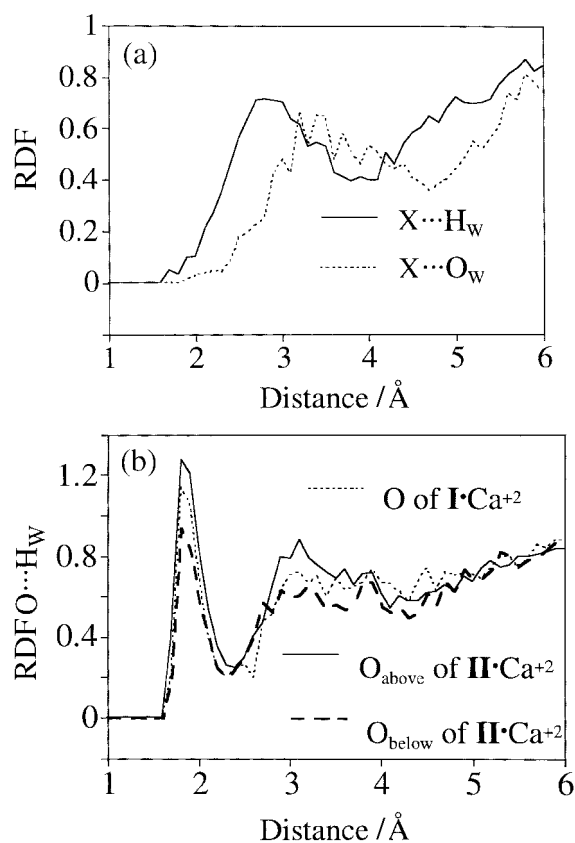
Fig. 7 (*a*) Radial distribution functions $X\cdots O_W$ and $X\cdots H_W$, where X is the center of mass of the oxygen atoms which coordinate the cation in **I**·Ca²⁺ (type **1**). (*b*) Radial distribution functions $O\cdots H_W$, calculated for **I**·Ca²⁺ (type **1**) and **II**·Ca²⁺ (type **1**). Two types of coordinating oxygen atoms in **II**·Ca²⁺ (type **1**) have been distinguished: those which lie "above" (O_{above}) or "below" (O_{below}) the average plane of coordinating oxygen.

Hydration patterns. For the complexes, unlike the free ligands, no hydrogen bonding is observed between the solvent and the nitrogen atoms of the ligand, the closest contacts with water being 4 Å (Fig. 6). This is an expected consequence of the involvement of the nitrogen lone pairs in coordination to the metal cation. RDF calculations show that non-coordinated O atoms form three hydrogen bonds with water, as for the free ligands, but each of the coordinated oxygens forms on average only one hydrogen bond with water (Fig. 7a,b). Differences arise between hydration patterns for adjacent coordinating O atoms for the M_I form of **II**·Ca²⁺ (type **1**) (Fig. 7b) as they are in a nonplanar arrangement. The O atoms "above" the average

plane of the binding oxygens are better solvated than the two "below". Fig. 7b also shows that binding oxygens in $I \cdot Ca^{2+}$ (type 1) are hydrated better than the "upper" oxygens and less than the "lower" oxygens of $II \cdot Ca^{2+}$ (type 1). All studied stereoisomers of $I \cdot Ca^{2+}$ (type 1) are found to be similarly hydrated (Table 3).

Unlike $I \cdot Ln^{3+}$ complexes,[9–11] no water molecules directly coordinate to the cation in the $I \cdot Ca^{2+}$ (type 1) complex.

Hydration patterns in $I \cdot Ca^{2+}$ (type 1) and $II \cdot Ca^{2+}$ (type 1) differ. In the $I \cdot Ca^{2+}$ (type 1) complex, one water molecule "bridges" two adjacent oxygen atoms, whereas in $II \cdot Ca^{2+}$ (type 1) such "bridges" are formed both between two adjacent and between two opposite oxygens (Fig. 5).

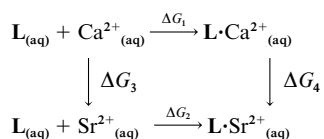### 3.3 L·Sr²⁺ Complexes in the gas phase and in water

Since the type 1 form was found to be much more stable than others for the $L \cdot Ca^{2+}$ complexes, only these conformers of I and II (M_1 forms) were simulated in the gas phase and in water for the $L \cdot Sr^{2+}$ complexes. The structures of the complexes after 300 ps of simulation time are shown in Fig. 8, and geometry and energy parameters are given in Tables 2 and 3. In the gas phase, the cation in the $L \cdot Sr^{2+}$ complexes is eight coordinated. The $I \cdot Sr^{2+}$ complex looks similar to its calcium analog, but in $II \cdot Sr^{2+}$, unlike $II \cdot Ca^{2+}$, the four coordinating oxygen atoms lie in the same plane.

In water, as for the $L \cdot Ca^{2+}$ complexes, longer (by 0.05 Å) Sr^{2+}–O and shorter (by 0.06 Å) Sr^{2+}–N distances are observed in $L \cdot Sr^{2+}$, compared to the gas phase structures. These changes result from repulsive interactions between water and the cation.

The hydration patterns of $I \cdot Sr^{2+}$ and $II \cdot Sr^{2+}$ differ. In $II \cdot Sr^{2+}$ the cation coordinates to one water molecule taking up the ninth coordination site of Sr^{2+}, whereas no water molecule is observed in the first coordination shell of $I \cdot Sr^{2+}$ (Fig. 8). As a result, the cation–water interaction energy is higher by 27 kcal mol^{-1} for I. It contrasts with the $I \cdot Ca^{2+}$ and $II \cdot Ca^{2+}$ (type 1) complexes where the Ca^{2+}–water interaction energy, $E_{ML \cdots w}$, is found to be similar, because of the similarity of their hydration patterns.

3.4 Free energy calculations on L·M²⁺ complexes: Ca²⁺ vs. Sr²⁺ binding

The thermodynamic cycle shown in Scheme 1 allows the

$$
\begin{array}{ccc}
L_{(aq)} + Ca^{2+}_{(aq)} & \xrightarrow{\Delta G_1} & L \cdot Ca^{2+}_{(aq)} \\
\downarrow \Delta G_3 & & \downarrow \Delta G_4 \\
L_{(aq)} + Sr^{2+}_{(aq)} & \xrightarrow{\Delta G_2} & L \cdot Sr^{2+}_{(aq)}
\end{array}
$$

Scheme 1

calculation of the binding selectivity $\Delta\Delta G_C$ of L in solution for ions. The selectivity is measured experimentally by $\Delta G_1 - \Delta G_2$ and is calculated via the "alchemical route" as $\Delta\Delta G_C = \Delta G_3 - \Delta G_4$.[43] In this cycle, ΔG_4 corresponds to the differences between free energies of the $L \cdot Ca^{2+}/L \cdot Sr^{2+}$ complexes in solution and ΔG_3 is the difference in hydration energies between Ca^{2+} and Sr^{2+} uncomplexed. Thus, the complexation selectivity is an interplay between intrinsic stability of $L \cdot Ca^{2+}$ and $L \cdot Sr^{2+}$ complexes and hydration energies of uncomplexed cations. The calculated value of ΔG_3 (37.3 kcal mol^{-1}, Table 4) agrees reasonably well with the experimental one (34.9 kcal mol^{-1}).[32]

The calculations were performed on the conformers 1 (M_1 form) and 2 of I and on the conformer 1 of II. The ΔG_4 energies (Table 4) clearly show a large intrinsic preference of both ligands for Ca^{2+}, which overcomes the unfavorable ΔG_3 term. The relative complexation free energies $\Delta\Delta G_C$ calculated according to Scheme 1 lead to a Ca^{2+} selectivity both for I and II. Qualitatively, this corresponds to experimental observ-

Table 4 Calculated free energy differences between Ca^{2+} and Sr^{2+} complexes of I and II in water[a]

Ligand	I		II
Complex type	1	2	1
ΔG_3	37.3/37.2	37.3/37.2	37.3/37.2
ΔG_4	51.2/51.2[c]	46.5/46.2	45.5/45.7
$\Delta\Delta G_C$	−13.9	−9.1	−8.3
$\Delta\Delta G_C$(exp)[b]	−2.7		−3.6

[a] The two numbers given for ΔG_3 and ΔG_4 correspond to the forward and backward free energies. [b] Experimental values for ref. 17. [c] Calculations performed on the M_1 form of $I \cdot Ca^{2+}$ (type 1).

ations,[17] although the calculated values are found to be larger than the experimental ones (Table 4). The reason for such a large deviation between calculations and experiment might be explained by neglecting in our simulations polarization and charge transfer effects. Due to polarization effects,[30] in the presence of cation the charges on coordinating oxygens become more negative and those on non-coordinating oxygens become less negative, whereas in MD and FEP simulations on the $L \cdot M^{2+}$ complexes these charges were taken to be the same. Charge transfer from the anionic ligand to M^{2+} reduces the positive charge of the cation and, thus, may also modify calculated free energies.

4 Discussion

4.1 Structure of I·Ca²⁺ in aqueous solution vs. solid state structure

In the solid state structure of the $I \cdot 2Ca^{2+}$ complex,[34] the cations occupy both endo and exo positions with respect to the ligand's pseudocavity. The endo coordinated cation is situated in the pseudocavity formed by four nitrogen atoms and four carboxylate oxygens (one oxygen atom per carboxylate group). The exo cation coordinates to two neighboring ligands and to three co-crystallized water molecules which do not form any hydrogen bonds with the donor atoms of I.

From our simulations in water, only the 1:1 complex appears to be stable. The neutral $I \cdot 2Ca^{2+}$ complex rapidly dissociated into $I \cdot Ca^{2+}$ and Ca^{2+} species. In the 1:1 complex, the geometry parameters of the ligand are similar within statistical fluctuations to those found in the solid state. Water molecules form hydrogen bonds with the oxygen atoms of carboxylate groups. Their interaction with the encapsulated Ca^{2+} is therefore repulsive, resulting in a slight shift of the cation toward the plane of nitrogen atoms. These hydration patterns differ from those for the lanthanide complexes of I which contain one inner-shell water molecule.[9–11]

Our simulations show the possibility of conformational exchange between different stereoisomers of the $I \cdot Ca^{2+}$ complexes. Thus, a transformation of the m_2 form into the M_2 form (Fig. 1) has been observed in water. Interestingly no isomerization was observed in the gas phase simulations and this implies that water catalyzes the interconversion of isomers. Although the M forms are about 9 kcal mol^{-1} more stable than the m ones (see E_{MLW} energies, Table 3), no firm conclusion about their relative stability in solution can be drawn since this energy difference is of the same order of magnitude as statistical fluctuations. It is possible that both forms are present in solution as in the case of some lanthanide complexes.[9–11]

4.2 Relative binding affinity of I and II for Ca²⁺

In this section, we analyze why I is a better Ca^{2+} binder than II. One possible approach would be to perform direct FEP calculations of relative I / II ligands selectivity for Ca^{2+}. This is a
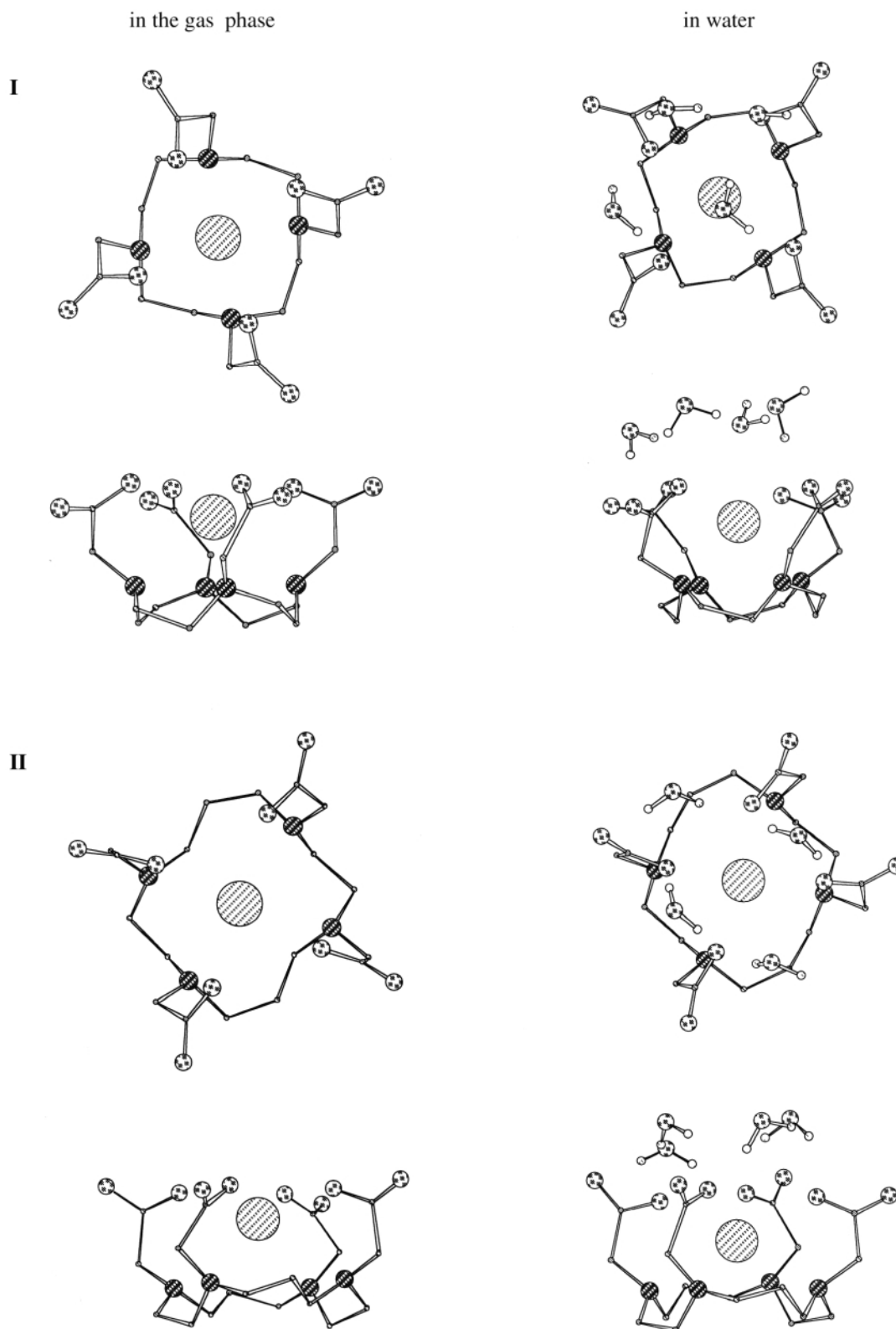
Fig. 8 Structure of **I·Sr²⁺** and **II·Sr²⁺** complexes after 300 ps of molecular simulation in the gas phase and in water. Water molecules that are within 4 Å of the center of mass of the O atoms bound to Sr²⁺ have been included. Top (first line) and side (second line) views.

more difficult task than calculations of Ca²⁺/ Sr²⁺ selectivity of **L**, because they would involve mutation of one molecule to another one.[43] A simpler method to obtain some qualitative insights into this question can come from the examination of the interaction energies and their components (Tables 1 and 3). Such an approach is justified by the fact that enthalpies of complexation of **I** and **II** with Ca²⁺and Sr²⁺ follow the same trend as the complexation free energies.[44] Analogously, a linear correlation between experimental entropies and free energies has been observed for a number of complexation processes

involving metal cations and macrocyclic ligands and their analogs.[45–47]

The energy ($E_{comp,L}$) of complexation (eqn. (4)) of the ligand

$$(L)_{aq} + (M^{2+})_{aq} \longrightarrow (L \cdot M^{2+})_{aq} \qquad (4)$$
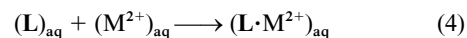
L with M²⁺ in water is expressed as $E_{comp,L} = E_{MLW} - E^0_{LW} - E_M + \Delta E_{WW}$, where E_{MLW} (Table 3) and E^0_{LW} (Table 1) are calculated according to eqns. (3) and (2), respectively, ΔE_{WW} is the solvent reorganization energy, and E_M is the cation

hydration energy. The E^0_{LW} and E^0_L energies correspond to uncomplexed **L**.

Taking into account that E_{MLW} is a sum of the cation–ligand interaction energy ($E_{M\cdots L}$), ligand steric energy (E_L), and hydration energy of the complex ($E_{ML\cdots W}$), $E_{MLW} = E_{M\cdots L} + E_L + E_{ML\cdots W}$, and E^0_{LW} is a sum of steric energy of uncomplexed **L** (E^0_L) and its hydration energy ($E^0_{L\cdots W}$), one can derive eqn. (5).

$$E_{\text{comp},L} = (E_L - E^0_L) + (E_{ML\cdots W} - E^0_{L\cdots W}) + E_{M\cdots L} - E_M + \Delta E_{WW} \quad (5)$$

When two ligands are compared, one may estimate the difference $\Delta E_{I,II}$ between the corresponding $E_{\text{compl},I}$ and $E_{\text{compl},II}$ complexation energies. Assuming that solvent reorganization energies ΔE_{WW} are similar for **I** and **II**, one can derive $\Delta E_{I,II}$ from eqns. (4) and (5) as the following:

$$\Delta E_{I,II} = E_{\text{compl},I} - E_{\text{compl},II} = \Delta(E_L - E^0_L) + \Delta(E_{ML\cdots W} - E^0_{L\cdots W}) + \Delta E_{M\cdots L} \quad (6)$$

where Δ means a difference between the corresponding energy components for **I** and **II**.

Calculations according to eqn. (6) were performed using the data from Tables 1 and 4 for the most stable conformers in water: type **1** for the **L·Ca²⁺** complexes, type **2** for uncomplexed **I** and type **1** for uncomplexed **II**. The calculated $\Delta E_{I,II}$ energy difference is close to zero, which is difficult to interpret because of relatively large statistical fluctuations in the energy terms reported in Table 3. A qualitative explanation of the relative binding efficiency of **I** vs. **II** can, nonetheless, be done analyzing energy components of $\Delta E_{I,II}$. As follows from eqn. (6), only three factors influence the **I/II** calcium selectivity: cation–ligand interactions (via $E_{M\cdots L}$), hydration effects (via $E_{ML\cdots W} - E^0_{L\cdots W}$) and steric effects (via $E_L - E^0_L$).

The cation–ligand energies $E_{M\cdots L}$ are similar in **I·Ca²⁺** and **II·Ca²⁺** complexes (Table 3), where the cation is similarly coordinated. Thus, the relative **I/II** complexation selectivity may result from an interplay between hydration and steric energy terms in eqn. (6).

The solvation term, $E_{ML\cdots W} - E^0_{L\cdots W} = E_{L\cdots W} + E_{M\cdots W} - E^0_{L\cdots W}$, gives a preference of 30 kcal mol⁻¹ for **II**. Indeed, hydration energies of uncomplexed macrocycles **I** and **II** ($E^0_{L\cdots W}$, Table 1), as well as the cation in the **L·Ca²⁺** complexes ($E_{M\cdots W}$, Table 3) are similar, but the complexed ligand **II** is 43 kcal mol⁻¹ better solvated than **I** ($E_{L\cdots W}$, Table 3) roughly due to the contribution of the carboxylatomethyl arms to $E_{L\cdots W}$. The macrocyclic fragment is similarly hydrated in both ligands, whereas hydration of carboxylates is much more efficient in **II·Ca²⁺** than in **I·Ca²⁺**. This is attributed to the different hydration patterns of the complexes: in **I·Ca²⁺** one water molecule "bridges" two adjacent oxygen atoms, whereas in **II·Ca²⁺** (type **1**) such "bridges" are formed both between adjacent and opposite oxygens (Fig. 5).

The ligand strain energy induced upon Ca²⁺ complexation, $E_L - E^0_L$ (Tables 1 and 3), is 31 kcal mol⁻¹ more favorable for **I**. The energy component analysis shows that the intramolecular electrostatic interactions, mostly between negatively charged N atoms of the macrocyclic backbone, provides the greatest resistance to conformational change from the free ligand to the complex. The decrease in $N\cdots N$ distances upon complexation is roughly twice as large for **II** (0.7 Å between the adjacent nitrogens and 1.2 Å between the opposite ones) than for **I** (0.4 Å between the adjacent nitrogens and 0.6 Å between the opposite ones).

Experimentally, ligand **I** displays higher binding affinity for Ca²⁺ than **II** in water. Since the relative steric energy, $E_L - E^0_L$, is the only term in eqn. (6) which leads to a preference of **I** over **II** for Ca²⁺, we explain the better complexation properties of **I** compared to **II** by its better preorganization for complexation.

Conclusions

Molecular dynamics and free energy perturbation simulations have been performed in the gas phase and in water on uncomplexed macrocyclic anions (**L**) DOTA **I** and TETA **II**, as well as on their complexes with alkaline earth cations M²⁺ (M²⁺ = Ca²⁺, Sr²⁺). We have found that in water both ligands form 1:1 complexes. Different conformers of **L·M²⁺** were simulated in water. The most stable type **1** complex corresponds to M²⁺ situated in a pseudocavity formed by four nitrogen atoms of the macrocyclic backbone and four oxygens of carboxylate groups, as found in the solid state structure of the complex of **I** with Ca²⁺. In aqueous solution, in contrast to the lanthanide complexes of **I**, in **L·M²⁺** there are no water molecules directly coordinated to the complexed cation. The first shell water molecules form hydrogen bonds with the oxygens of carboxylate groups and repulsively interact with M²⁺, shifting the cation toward the macrocyclic ring of **L**. An exchange of stereoisomers of the **I·Ca²⁺** complex was observed in water but not in the gas phase, showing that solvent may catalyze conformational transitions in the metal complexes of **L**. Both **I** and **II** display larger intrinsic affinity for Ca²⁺ than for Sr²⁺ which explains their selectivity for Ca²⁺ in water. The higher stability of **I·Ca²⁺** over **II·Ca²⁺** complexes is explained by the better preorganization of **I**, which loses less conformational energy than **II** upon complexation with the cation.

References

1 J.-F. Desreux, *Inorg. Chem.*, 1980, **19**, 1319.
2 M. R. Spirlet, J. Rebizant, J.-F. Desreux and M. F. Loncin, *Inorg. Chem.*, 1984, **23**, 359.
3 M. F. Loncin, J.-F. Desreux and E. Merciny, *Inorg. Chem.*, 1986, **25**, 2646.
4 V. Alexander, *Chem. Rev.*, 1995, **95**, 273 provides a brief overview.
5 M. F. Tweedie, in *Lanthanide Probes in Life, Chemical and Earth Sciences*, ed. G. R. Choppin and J.-C. G. Bünzli, Elsevier, New York, 1989, ch. 3.
6 C. A. Chang, L. C. Francesconi, M. F. Malley, K. Kumar, J. Z. Gougoutas, M. F. Tweedie, D. W. Lee and L. J. Wilson, *Inorg. Chem.*, 1993, **32**, 3501.
7 K. Kumar, C. A. Chang, L. C. Francesconi, D. D. Dischino, M. F. Malley, J. Z. Gougoutas and M. F. Tweedie, *Inorg. Chem.*, 1993, **33**, 3567 and references therein.
8 D. E. Reichert, J. S. Lewis and C. J. Anderson, *Coord. Chem. Rev.*, 1999, **184**, 3.
9 S. Aime, M. Botta, M. Fasano, M. P. M. Maques, C. F. G. C. Geraldes, D. Pubanz and A. E. Merbach, *Inorg. Chem.*, 1997, **36**, 2059.
10 R. S. Dickens, J. A. K. Howard, C. L. Maupin, J. M. Moloney, D. Parker, R. D. Peacock, J. P. Riehl and G. Siligardi, *New J. Chem.*, 1998, 891.
11 S. Aime, A. Barge, J. Bruce, M. Botta, J. A. K. Howard, J. M. Moloney, D. Parker, A. S. de Sousa and M. Woods, *J. Am. Chem. Soc.*, 1999, **121**, 5762.
12 R. B. Martin and F. S. Richardson, *Quart. Rev. Biochem.*, 1979, **12**, 181.
13 J.-C. G. Bünzli, in *Lanthanide Probes in Life, Chemical and Earth Sciences*, ed. G. R. Choppin and J.-C. G. Bünzli, Elsevier, New York, 1989, ch. 7, pp. 21.
14 S. L. Wu, K. A. Johnson and W. deW. Horrocks, *Inorg. Chem.*, 1997, **36**, 1884.
15 H. Stetter and W. Frank, *Angew. Chem., Int. Ed. Engl.*, 1976, **15**, 686.
16 W. P. Cacheris, S. K. Nickle and A. D. Sherry, *Inorg. Chem.*, 1987, **26**, 958.
17 R. Delgado and J. J. R. Frausto da Silva, *Talanta*, 1982, **29**, 815.
18 (CSD Refcode) CEXKUL, Na[Eu(DOTA)(OH₂)]·4H₂O (Ref. 2); JOPJIH01, Na[Gd(DOTA)(OH₂)]·4H₂O (Ref. 6)); LATKOG, Na-

[Y(DOTA)(OH$_2$)]·4H$_2$O (Ref. 6); LATKAS, Na[Fe(DOTA)]·5H$_2$O (Ref. 6); ZUGTAX, [Ca(OH$_2$)$_3$]$_2$[Ca(DOTA)]$_2$·15.4H$_2$O (Ref. 34).

19 U. Cosentino, G. Moro, D. Pitea, A. Villa, P. C. Fantucci, A. Maiocchi and F. Uggeri, *J. Phys. Chem. A*, 1998, **102**, 4606.
20 J. H. Forsberg, R. M. Delaney, Q. Zhao, G. Harakas and R. Chandran, *Inorg. Chem.*, 1995, **34**, 3705 and references therein.
21 C. Lecomte, V. Dahaoui-Gindrey, H. Chollet, C. Gros, A. K. Mishra, F. Barbette, P. Pullumbi and R. Guilard, *Inorg. Chem.*, 1997, **36**, 3827 and references therein.
22 R. Fossheim and S. G. Dahl, *Acta Chem. Scand.*, 1990, **44**, 698.
23 R. Fossheim, S. G. Dahl and H. Dugstad, *Eur. J. Med. Chem.*, 1991, **26**, 200.
24 R. Fossheim, H. Dugstad and S. G. Dahl, *J. Med. Chem.*, 1991, **34**, 819.
25 D. E. Reichert, R. D. Hancock and M. J. Welch, *Inorg. Chem.*, 1996, **35**, 7013.
26 D. A. Pearlman, D. A. Case, J. C. Caldwell, W. S. Ross, T. E. Cheatham III, D. M. Ferguson, G. L. Seibel, U. C. Singh, P. K. Weiner and P. A. Kollman, AMBER4.1, University of California, CA, 1995.
27 S. J. Weiner, P. A. Kollman, D. T. Nguyen and D. A. Case, *J. Comput. Chem.*, 1986, **7**, 230; W. D. Cornell, P. Cieplak, C. I. Bayly, I. R. Gould, K. M. Merz, D. M. Ferguson, D. C. Spellmeyer, T. Fox, J. W. Caldwell and P. A. Kollman, *J. Am. Chem. Soc.*, 1995, **117**, 5179.
28 SPARTAN, Version 4.1, Wavefunction Inc., Irvine, CA, 1996.
29 R. V. Stanton, L. R. Little and K. M. Merz, *J. Phys. Chem.*, 1995, **99**, 483.
30 Energy minimization of **I** and its type **1** complexes with Ca^{2+} and Sr^{2+} were performed using hybrid quantum mechanics/molecular mechanics (QM/MM) method[29] using the ROAR program.[50] In these calculations, for the ligand we used PM3 semi-empirical method,[51] whereas cations were treated classically, as in purely force field calculations, using the AMBER4 force field[26] to estimate its non-bonded interactions with the ligand. In such a way, there is no charge transfer from the ligand but polarization of the latter in the field of the cation was taken into account.

   In the uncomplexed tetraanion **I** the negative Mulliken charges on the oxygen atoms (-0.67) are larger than on the N atoms (-0.07). In the **I·M^{2+}** complexes, the cation induces some changes in the charge distribution of the ligand. The charges on the carboxylic oxygens become different (-0.77 on the atoms coordinating to M^{2+} and -0.57 on non-coordinating atoms) although their average value remains the same as in the uncomplexed **I**. The negative Mulliken charges on nitrogens increase to -0.14. Thus, polarization effects diminish the difference between the average charges on O and N atoms and qualitatively, at least, this corresponds to the modifications made on the initial set of ESP charges reported in the section Fitting of parameters.

31 S. Durand, *Simulations par mécanique quantique et dynamique moléculaire de la complexation de cations alcalino-terreux et lanthanides par des ligands polyaminocarboxylate*, Doctoral Thesis, Strasbourg, 1999.
32 J. Åqvist, *J. Phys. Chem.*, 1990, **94**, 8021.
33 A. D. MacKerell, D. Bashford, M. Bellott, R. L. Dunbrack, J. D. Evanseck, M. J. Field, S. Fischer, J. Gao, H. Guo, S. Ha, D. Joseph-McCarthy, L. Kuchnir, K. Kuczera, F. T. K. Lau, C. Mattos, S. Michnick, T. Ngo, D. T. Nguyen, B. Prodhom, W. E. Reiher and B. Roux, *J. Phys. Chem. B*, 1998, **102**, 3586.
34 O. P. Andersen and J. H. Reibenspies, *Acta Crystallogr.*, *Sect. C*, 1996, **52**, 792.
35 MacroModel 5.5, Columbia University, New York, 1996.
36 M.-R. Spirlet, J. Rebizant, M.-F. Loncin and J.-F. Desreux, *Inorg. Chem.*, 1984, **23**, 4278.
37 A. Riesen, M. Zehnder and T. A. Kaden, *Acta Crystallogr.*, *Sect. C*, 1991, **47**, 531.
38 D. Q. McDonald and W. C. Still, *J. Am. Chem. Soc.*, 1994, **116**, 11550.
39 J. R. Morrow, S. Amin, C. H. Lake and M. R. Churchill, *Inorg. Chem.*, 1993, **32**, 4566.
40 W. L. Jorgensen, J. Chandrasekhar and J. D. Madura, *J. Chem. Phys.*, 1983, **79**, 926.
41 U. C. Singh, F. K. Brown, P. A. Bash and P. A. Kollman, *J. Am. Chem. Soc.*, 1987, **109**, 1607.
42 A. Varnek, E. Engler, M. Lauterbach, L. Troxler and G. Wipff, in *Crystallography of Supramolecular Compounds*, ed. G. Tsoucaris, J. L. Atwood and J. Lipkowski, *NATO ASI Ser.*, Dordrecht, Boston, London, 1996, pp. 465–470.
43 P. Kollman, *Chem. Rev.*, 1993, **93**, 2395.
44 R. Delagado, J. J. R. Frausto da Silva and M. C. T. A. Vaz, *Inorg. Chim. Acta*, 1984, **90**, 185.
45 Y. Inoue, Y. Liu and T. Hakushi, in *Cation Binding by Macrocycles*, ed. Y. Inoue and G. W. Gokel, Marcel Dekker, Inc., N Y, Basel, 1990, pp. 1–110.
46 Y. Inoue, T. Hakushi, Y. Liu, L.-H. Tong, B.-J. Shen and D.-S. Jin, *J. Am. Chem. Soc.*, 1993, **115**, 475.
47 A. Y. Tsivadze, A. A. Varnek and V. E. Khutorsky, *Coordination Compounds of Metals with Crown-Ligands* (*Russ.*), Moscow, 1991.
48 E. J. Corey and J. C. Bailar, *J. Am. Chem. Soc.*, 1959, **81**, 2620.
49 J. K. Beattie, *Acc. Chem. Res.*, 1971, **4**, 253.
50 A. Cheng, R. S. Stanton, J. J. Vincent, K. V. Domodaran, S. L. Dixon, D. S. Hartsough, M. Mori, S. A. Best and K. M. Merz, ROAR 1.0 program, Pennsylvania State University, 1997.
51 J. J. P. Stewart, *J. Comput. Chem.*, 1989, **10**, 209.

Paper 9/06981J